TELKOMNIKA Indonesian Journal of Electrical Engineering
Vol. 12, No. 5, May 2014, pp. 3920 ∼ 3927
DOI: http://dx.doi.org/10.11591/telkomnika.v12.i5.4390

Image Deformation Based on Wavelet Filter and Control Curves

Hong-an Li[1*], Jie Zhang[2], and Baosheng Kang[1]
[1]School of Information Science and Technology, Northwest University, Xi'an 710127, China
[2]Department of Hematology, Tangdu Hospital, Fourth Military Medical University, Xi'an 710038,China
[*]corresponding author, e-mail: an6860@126.com

Abstract

We provide an image deformation method based on wavelet filter using control curves and moving least squares. The image is preprocessed firstly instead of being directly deformed by the old ways. And the original image will be filtered into a high frequency part and a low frequency part by the wavelet, and then use the moving least squares and the control curves only to deform the low frequency part, but not the high frequency part. The key points are set to create control curves according to shape information or deformation requirement, and moved to new position to deform the image using moving least squares. The final result of image deformation is obtained by adding the deformed low frequency part to the high frequency part of the original image. Experiments show that the high frequency detail information is well preserved and the image shape and contour are also well described, and so the deformation results are satisfactory and realistic.

Keywords: *Image Deformation, Wavelet Filter, Moving Least Squares, Control Curves*

1. Introduction

The image deformation technology is widely applied in the fields of television animation [1] and medical image processing [2], etc. The familiar image deformation method is that some control objects are chosen to control the deformation, which can be control points [3], line segments or polygon meshes [4]. The image deformation is carried out through changing the positions of the control objects.

Many scholars have put forward image deformation methods, and the main difference of those methods is that their deformation control objects are different. Lee presented the free grid deformation technology [5], which achieves deformation by the image parameterization based on binary cubic interpolation spline, and the default of this method is that it needs to align the register grid according to image characteristics with the control point spline. Beier and Neely improved the free grid deformation technology by using a set of line segments to control the deformation, which is convenient for users [6]. Koba used the improved free grid deformation technology in the image surface deformation and achieved a good deformation result [7]. Igarashi put forward point-based image deformation method [8], in which the input image is subdivided into triangles and to solve the system of linear equations with the its number of unknown variables equal to the number of all triangle vertexes, in order to reduce the distortion degree of the deformed image and keep image deformation as rigid as possible. A common characteristic of the above deformation methods is to minimize their local scaling and shearing, but these deformation operations are complicated and the realistic effect of deformation is not very good.

Literature [9] proposed an image deformation method based on Moving Least Squares (MLS), in which a deformation mapping function of feature points or segments are established and used to control different image deformations. The deformation method has good realistic effect and enables users to feel like manipulating real objects. But it is apt to produce bad results with shear, distortion and stretch with wrong proportion, and its deformation effect is often not ideal in some local locations with the same scale, so it has some limitations.

We propose an image method based on wavelet filter using control curves and MLS. Firstly, the image is preprocessed and filtered out the high frequency part. Then only the low

Received October 10, 2013; Revised December 7, 2013; Accepted January 2, 2014

frequency part is deformed using the control curves and MLS. Finally, the deformed low frequency part is added to the high frequency part, thus the realistic image deformation is realized.

2. Image Deformation Using MLS

The MLS deformation technology regards the image before deformation as an independent variable, the deformed image as target variable, and the whole process of deformation algorithm is to find the mapping function f. Fig. **??** is the original image and Fig. **??** is the corresponding deformed image, which is obtained by employing deformation function f.

[Original]  [Deformed] 

Figure 1. Image deformation

According to MLS theoretical model [8], with set S as the feature points set of original image and set D as the feature points set of deformed image, there is a deformation function f which can make the value of Eq. (1) minimum.

$$\sum w_i |f(s_i) - d_i|^2. \tag{1}$$

$$w_i = \frac{1}{|s_i - v|^2}. \tag{2}$$

Where, w_i is weight and its value varies according to the position of v in the image, and v stops moving when corresponding value of Eq. (1) is minimum, so the method is called MLS [9]. When v is equal to s_i , weight value w_i is infinite, so define $f(s_i) = d_i$; When feature point does not vary, define $f(s_i) = s_i = d_i$.

$$f(x) = xM + T. \tag{3}$$

Where, M represents linear transformation, and T represents translation transformation.

$$T = \sum_i w_i d_i / \sum_i w_i - \left(\sum_i w_i s_i / \sum_i w_i \right) M. \tag{4}$$

With Eq. (4) substituted into Eq. (3), we obtain:

$$f(x) = \left(x - \sum_i w_i s_i / \sum_i w_i \right) M + \sum_i w_i d_i / \sum_i w_i. \tag{5}$$

Set

$$\begin{cases} \hat{s}_i = s_i - \left(\sum_i w_i s_i / \sum_i w_i \right) \\ \hat{d}_i = d_i - \left(\sum_i w_i d_i / \sum_i w_i \right) \end{cases} \tag{6}$$

So Eq. (1) can be rewritten into:

$$\sum_i w_i |\hat{s}_i M - \hat{d}_i|^2. \tag{7}$$

The procedure of the MLS image deformation algorithm includes:

Step 1 Select feature points set $S = \{s_1, s_2, \cdots, s_n\}$ in the original image Fig. **??**.

Step 2 Determine the positions of in the deformed image Fig. **??**, which can be denoted as a new feature points set $D = \{d_1, d_2, \cdots, d_n\}$.

Step 3 Determine the mapping function f according to $d_i = f(s_i)$.

Linear transformation M can be affine transformation, similarity transformation and rigid transformation. The deformed image can be obtained by applying mapping f to the remaining points of original image. Forward mapping or reverse mapping can be used to generate a new image. Forward mapping is prone to produce voids and overlapping phenomena, so reverse mapping is adopted in this paper. The MLS image deformation effects are shown in Fig. 2 [9].

[Original]  [Affine]  [Similarity]  [Rigid] 

Figure 2. Image deformation based on MLS

Where, Fig. **??** is the original image, Fig. **??** is an affine deformed image, Fig. **??** is a similarity deformed image, and Fig. **??** is a rigid deformed image. There is serious wrong shear phenomenon and uneven scaling transformation in Fig. **??**. The effect of Fig. **??** is better than that of Fig. **??**, but there is proportional distortion in the right part of image in Fig. **??**. Fig. **??** is preferably and relatively similar to the deformation effect of real object, so rigid transformation is adopted in this paper.

[Original]  [Deformed]  [Deformed] 

Figure 3. Image rigid deformation

The most significant characteristic of the MLS image deformation method is simple and easy to realize. But it also has several defects, which are mainly reflected in following aspects. Firstly, it achieves good deformation effect only when dealing with point-based affine transformation. Secondly, in actual operation feature points set S may not be completely accurate mapping to the deformation feature points set D. Thirdly, there may be stretch phenomenon in deformed image as showed in Fig. **??** and Fig. **??**. Lastly, it does not consider that there exists a large number of unneeded operating points in the deformation process, which could be filtered out according to the intensity of the frequency variation, so the computational complexity of the MLS image deformation method is large, and there is real-time bottlenecks when the number of feature points is large.

3. Wavelet Filter

Wavelet transform is considered as a new milestone in the development of Fourier transform, which is regard as mathematical microscope with excellent "zoom" performance. In wavelet transform, signal is represented as a weighted sum of a series of basis functions, and basis functions are obtained from a wavelet mother function by dilation and translation. Wavelet function is a short-term shock function with compact support and it has local characteristics in the time domain, also being called as spatial domain, and frequency domain [10]. The joint analysis of spatial domain and frequency domain obtained from wavelet transform makes it to be a good tool to extract both detail components and approximate components of images, where the low frequent part of signal is considered as the approximate signal and the high frequent part is considered as the details of signal.

The original image is treated as a signal $f(t)$, which is filtered into different frequency components using Mallat algorithm [11], [12]:

$$f(t) = A_{j-1}f(t) = A_j f(t) + D_j f(t). \tag{8}$$

Where, $A_j f(t)$ is one component of signal $f(t)$, whose frequency is not past 2^{-j}; The frequency of $D_j f(t)$ is between 2^{-j} and 2^{-j+1}.

Eq. (8) is rewritten into a matrix form:

$$C_{j+1} = HC_j,\ D_{j+1} = GC_j \quad (j = 1, 2, \cdots, J). \tag{9}$$

Where, J is the wavelet decomposition level. Eq. (9) is the Mallat pyramidal decomposition algorithm, whose process is shown by Fig. 4. Where, $2\downarrow$ is the value of only even location.

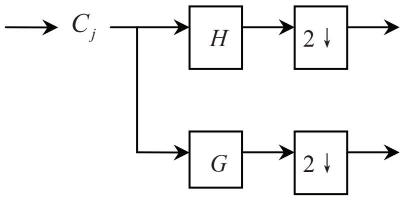

Figure 4. Decomposition of Mallat pyramidal algorithm

After $f(t)$ is decomposed according to the Mallat algorithm, the signal is distinguished from noise based on the experiential information, and then $f(t)$ is filtered to generate a new sequence C_j and D_j.

The Mallat reconfiguration algorithm is:

$$C_j = H^* C_{j+1} + G^* D_{j+1} \quad (j = J, J-1, \cdots, 1). \tag{10}$$

Where, the conjugates of H^* and G^* are H and G, whose process is shown in Fig. 5. Where, $\uparrow 2$ is the liter sample, it means that the number of samples is 2 times than the original.

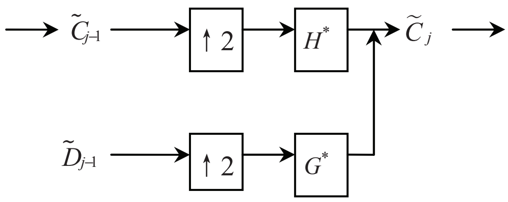

Figure 5. Reconstruction of Mallat pyramidal algorithm

When the signal is reconfigured, the part is deleted which is relative to the high frequency detail signal and corresponding to the noise, and then the filtered signal is obtained:

$$f(t) = A_j f(t) = \sum_{k \in Z} C_{J,k} \phi_{J,k}(t). \tag{11}$$

Eq. (11) is a smooth signal expression after $f(t)$ is filtered. It is equivalent to using a smooth curve to fit it [12]. The high and low frequency of image are used to measure the changing intensity of

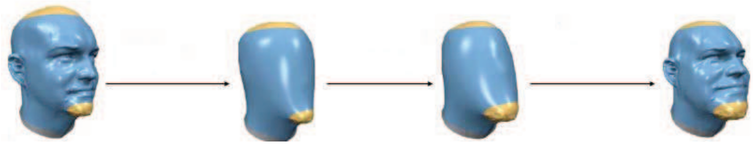

Figure 6. The process of image deformation based on wavelet filter using control curves and MLS

different locations. We use wavelet filter to filter out the high frequency part of image, and use the control curves and MLS to deform the low frequency part of the image. Then the final result of image deformation will appear by adding the deformed low frequency part to the high frequency part of the original image. The algorithm process is shown in Fig. 6.

4. Control Curves

In order to control the path of control curves, we use cubic spline curve fitting method to generate the control curves [13], [14]. Control points are piecewise fitted by cubic spline curve, and the curve can pass the control points accurately which has second order continuity on the connection point. We can get the control points by clicking the mouse. Assuming that we want to use $n+1$ orderly control points $a_j(j = 0,\ 1,\ 2,\ \cdots,\ n)$ to generate a curve which includes n segments. We use cubic spline curve to generate each segment, and the free endpoint conditions to generate the cubic spline curve. Suppose that $s_i(i = 0,\ 1,\ 2,\ \cdots,\ n)$ was the ith control curve before deformation, the $d_i(t)$ was the corresponding ith curve after the deformation, its corresponding $n+1$ ordered control points were $b_j(j = 0,\ 1,\ 2,\ \cdots,\ n)$, and $t \in (0,\ 1)$. According to Eq. (1) we can obtain:

$$\sum_i \int_0^1 w_i(t)|s_i(t)M + T - d_i(t)|^2 dt. \tag{12}$$

The equation of weight $w_i(t)$ is: $w_i(t) = \frac{|s'_i(t)|}{|s_i(t)-v|^{2a}}$. By getting the minimum value of Eq. (12) we can obtain:

$$T = d_* - s_* M. \tag{13}$$

The equation of s_* and d_* are:

$$s_* = \frac{\sum\limits_i \int_0^1 w_i(t)s_i(t)dt}{\sum\limits_i \int_0^1 w_i(t)dt} \qquad d_* = \frac{\sum\limits_i \int_0^1 w_i(t)d_i(t)dt}{\sum\limits_i \int_0^1 w_i(t)dt}. \tag{14}$$

Eq. (12) can be rewritten into:

$$\sum_i \int_0^1 w_i(t)|\hat{s}_i(t)M - \hat{d}_i(t)|^2 dt. \tag{15}$$

Where, $\hat{s}_i = s_i(t) - s_*$, $\hat{d}_i = d_i(t) - d_*$, $s_i(t)$and $d_i(t)$ are the curve segment of cubic spline curves respectively before and after image deformation, and the matrix expression of parameter variable equation, which is fitted interpolation by the cubic spline curve, is:

$$s_i(t) = (s_{ix}(t)\ \ s_{iy}(t)) = (t^3\ \ t^2\ \ t\ \ 1) \bullet \begin{vmatrix} 2 & -2 & 1 & 1 \\ -3 & 3 & -2 & -1 \\ 0 & 0 & 1 & 0 \\ 1 & 0 & 0 & 0 \end{vmatrix} \bullet \begin{vmatrix} a_{i-1} \\ a_i \\ a'_{i-1} \\ a'_i \end{vmatrix}. \tag{16}$$

a_{i-1} and a_i are respectively the start and end coordinates of the ith curve before image deformation, while a'_{i-1} and a'_i are respectively the first derivative values of start and end coordinates, and the value can be calculated by the free endpoints. In the same way, b_{i-1} and are respectively the start and end coordinates of the ith curve after image deformation, b'_{i-1} and b'_i are respectively the first derivative values of start and end coordinates.

According to Eq. (16), the expression of cubic spline curve can be rewritten into:

$$s_i(t) = (s_{ix}(t)\ \ s_{iy}(t)) = (t^3\ \ t^2\ \ t\ \ 1) \bullet (m_{1i}\ \ m_{2i}\ \ m_{3i}\ \ m_{4i})^T. \tag{17}$$

$$d_i(t) = (d_{ix}(t)\ \ d_{iy}(t)) = (t^3\ \ t^2\ \ t\ \ 1) \bullet (n_{1i}\ \ n_{2i}\ \ n_{3i}\ \ n_{4i})^T. \tag{18}$$

According to Eq. (17) and Eq. (18), we can generate cubic spline curve on the free endpoints, so the control curve set S and D are generated. Let the points in S match with the points in D, and use them as control points, and deform the image based on the control points set.

5. Experiments

5.1. Feature points extraction

According to the deformation requirement of face image in our experiment, we define 68 face feature points which refer to the definitions of face feature point parameters in MPEG-4 [15]. The face feature points mainly locate at outside contour of face, eyebrows, nose and mouth, and relatively dense feature points are set to the facial features region, which is the main part of deformation and action [16]. Facial feature points are divided into organ description feature points and basic feature points which are also called contour feature points. Basic feature points denoted as hollow dots in Fig. 7 describe the whole facial external characteristic, and they divide a whole face according to facial shape features and determine the characteristics of the face and the major organs, which is the important reference standard for establishing face deformation feature points.

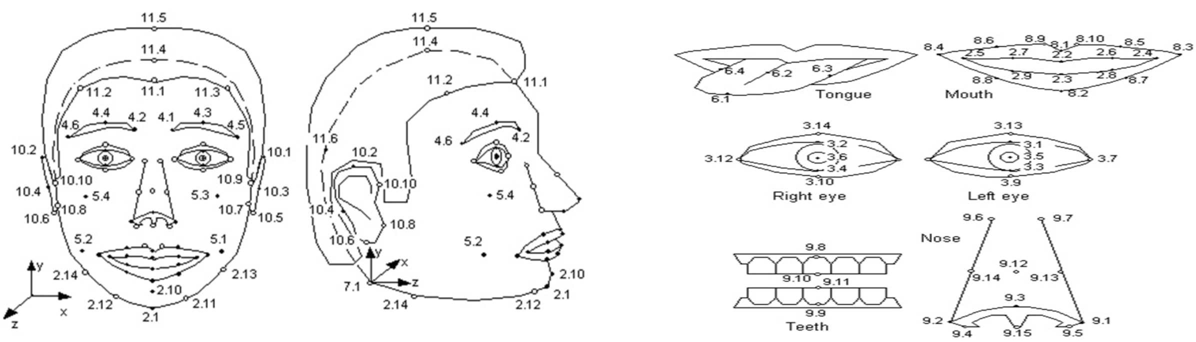

Figure 7. The MPEG-4 definition of the human face features

Only 13 points are set as the feature points in this paper, because those points cover the changing part of the smiling face and the effects of image deformation using the 13 points will be verified enough.

5.2. The algorithm of image deformation based on wavelet filter using control curves and MLS

Input a image needed to be deformed, and take the following steps to deform:

Step 1 Set key points to create a control curve set S, and the contour or shape of the image is represented.

Step 2 Move the points and change the position and direction of the spline curves to generate a control curve set D which has been deformed.

Step 3 Through calculation, make one-to-one correspondence between the control points of S and D to generate the control points.

Step 4 Filter the original image into a high frequency part and a low frequency part (Using the wavelet tool kit of the Matlab software).

Step 5 Deform the low frequency part of the image using the control points method.

Step 6 Add the deformed low frequency part to the high frequency part of the original image, and then the final result of image deformation will be obtained.

5.3. Experiment results

Matlab 2011b is adopted in the experiments, and the experiment results are shown in Fig. 8.

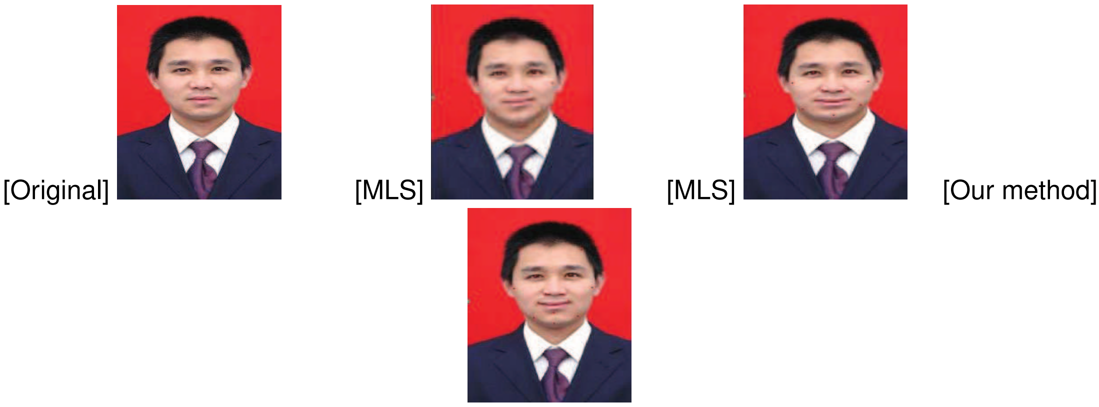

Figure 8. Image deformation results

The Fig. **??** is original image, the Fig. **??** and the Fig. **??** are the deformed images using MLS, and the Fig. **??** is the deformed image using our method. From the effect of the deformation we can see our method is good enough to keep the image details, and there is no local distortion and tension phenomenon as the Fig. **??** and the Fig. **??**, and our deformation is smooth and realistic. Because the high frequency part of the image has been filtered out, the differences between points in the low frequency part have been significantly reduced. Besides, during the deformation process, we don't deal with the high frequency information and only deal with the edge and contour of the image, retain the high frequency information completely. The control curve set is used to describe the shape topology relations or contour information, and the different parts of the contour and edge are deformed in different scales, so the different parts of the contour and edge can keep their shapes, and the final deformation effect will be more natural and smooth, so it can greatly improve the fitting effect using our method. At the same time it will reduce the number of feature points, so it can greatly increase the deformation speed.

6. Conclusions

We propose an image deformation method based on wavelet filter using control curves and MLS. In the aspects of complexity, deformation speed and the effect of the deformation are all improved using our method. Those mainly reflect in the following aspects: (1) The speed of algorithm and precision of calculation are improved, because only the low frequency part of the image is processed through the wavelet filtering; (2) The shape and contour of the image are well described, because different scales are taken to deform the different parts of the contour and edge of the image using control curves; (3) The high frequency information of the image is completely reserved, so the detail is clear and the deformation is smooth.

At present, the 3D model has been another important object to be dealt with in the field of visualization technology because of the rapid development of the computer hardware [17]. For the next work, the method of the this paper should be applied in the deformation of the 3D model in order to make it more smooth and natural.

Acknowledgement

This work is supported by the National Natural Science Foundation of China (No.61379010) and (No.61272286) .

References

[1] Smythe, D.B. A two-pass mesh warping algorithm for object transformation and image interpolation. Tech. Rep. 1030, ILM Computer Graphics Department, 1990.
[2] Bookstein, F. L. Thin-plate splices and the decomposition of deformations. IEEE Transactions on Pattern Analysis and Machine Intelligence, 1989; 11(6): 567-585.
[3] McCracken, R and Joy, K. I. Free form deformations with lattices of arbitrary topology. In Proceedings of ACM SIGGRAPH 1996, ACM Press, 1996; 181-188.
[4] Beier, T. and Neely, S. Feature based image metamorphosis. In SIGGRAPH 1992: Proceedings of the 19th annual conference on Computer graphics and interactive techniques, ACM Press, New York, USA, 1992; 35-42.
[5] Lee, S., Chwa, K. and Shin, S. Image metamorphosis using snakes and free-form deformations. In SIGGRAPH 1995: Proceedings of the 22nd annual conference on Computer graphics and interactive techniques, ACM Press, New York, USA, 1995; 439-448.
[6] Warren, J., Eechele, G., and Thaller, C., etc. A geometric database for gene expression data. ACM SIGGRAPH symposium on Geometry processing, 2003; 166-176.
[7] Koba yashi, K. and Otsubo, K. Free form deformation by using triangular mesh. Proceedings of the eighth ACM symposium on Solid modeling and applications, 2003; 226-234.
[8] Igarashi, T., Moscovich, T., and Hughes, J. F. As rigid as possible shape manipulation. ACM Trans. Graph. 2005; 24(3): 1134-1141.
[9] Schaefer, S.McPhail T. and Warren J. Image deformation using moving least squares. ACM Transactions on Graphics, 2006; 25(3): 533-540.
[10] FAN Chunnian, WANG Shuiping. Wavelet-based illumination normalization algorithm for face recognition. Computer Engineering and Applications, 2010; 46(6): 174-177.
[11] Zhang Xiangwei, Luo Shaoming, Zhong Tongzi. Wavelet Analysis in Testing Signal. Applied Mathematics and Mechanics, 1998; 19(3): 203-207.
[12] Ma Pan, Meng Lingkui, Wen Hongyan. Kalman Filtering Model of Dynamic Deformation Based on Wavelet Analysis. Geomatics and Information Science of Wuhan University, 2004; 29(4): 349-353.
[13] Hua Shungang, Li Xiaoxiao, Li Shaoshuai. Image Deformation Using Control Curves and Moving Least Squares. Journal of Chinese Computer Systems, 2010; 31(11): 2251-2254.
[14] Hua Shungang, Liu Ting. Study on image deformation based on moving least squares. Journal of Computer Applications, 2009; 29(1): 71-73.
[15] ISO/IEC JTC1/SC29 Document N3908, MPEG4 Video Verification Model version 18.0, 2001.
[16] Beibei Li, Qiang Zhang, etc. Facial Animation Based on Feature Points. TELKOMNIKA, March 2013; 11(3): 1697-1706.
[17] Guangguo Zhang, Jing Sheng, Feng Wang. A Finite Element Analysis of The Rectangle Spline Broach. TELKOMNIKA, December 2012; 10(8): 2125-2130.